

Monitoring of polymerization-induced phase separation by simultaneous photo-d.s.c./turbidity measurements

J. G. Kloosterboer*, C. Serbutoviez and F. J. Touwslager

Philips Research Laboratories, Prof. Holstlaan 4, 5656 AA Eindhoven, The Netherlands

(Received 29 May 1996)

Polymer-dispersed liquid crystals (PDLCs) can be used in displays. They can be made by polymerization-induced phase separation in a mixture of monomer and LC. Modification of a photo-d.s.c. with a laser and a photodiode enables the simultaneous measurement of heat flux and turbidity during polymerization. The heat flux yields the rate and conversion of the polymerization process, whereas turbidity indicates the appearance of a nematic phase. In this way the influence of the LC structure and content, the rate and temperature of polymerization and the cross-linker concentration on the phase separation process have been established for a simple model system. Recording of transmission-temperature curves before and after polymerization reveals the position of cloud points or clearing points in the phase diagram. The use of special cells allows the measurement of transmission-voltage curves on the d.s.c. samples after polymerization. The morphology, which is important with respect to electro-optical performance, strongly depends on the cross-link density at phase separation. Secondary phase separation inside LC domains already separated by cooling has been observed with microscopy during fast polymerization, not during slow reaction. Copyright © 1996 Elsevier Science Ltd.

(Keywords: PDLC; phase separation; photopolymerization)

Introduction

In polymer-dispersed liquid crystal display (PDLCs), microdroplets of LC material are embedded in a polymeric matrix. This matrix is confined between two glass plates coated with transparent electrodes. In the off-state the cell is highly opaque due to strong light scattering. The LC molecules in the droplets can be oriented by an external electric field. By application of an external electric field, the cell switches to transparent in the direction of the field through orientation of the LC molecules. One way of making these devices is to polymerize a solution of a multifunctional monomer in an LC solvent¹. The electro-optical response of these systems has been found to depend strongly on a variety of parameters, such as the monomer functionality, the structure and initial concentrations of monomer and LC and the rate and temperature of polymerization. All of these will affect the morphology of the phases since the latter depends on the relative rates of polymerization and phase separation. The morphology is also strongly influenced by the extent of reaction at which the phase separation sets in, since the presence of polymer will restrict the possibilities for growth of liquid phase domains. However, to the best of our knowledge the polymer content at phase separation does not seem to have been determined in systems of interest.

The generally accepted picture is that phase separation is induced by the increasing incompatibility of the growing polymer chains with the LC solvent. Droplets containing LC and monomer are formed, and these grow until their growth is arrested by gelation, then purification of the droplets occurs through consumption of

dissolved monomer by the polymerizing matrix. During this purification process the droplets will reach their nematic state¹. So far, the phase separation induced by cross-linking polymerization of, for example, epoxide/amine mixtures has mainly been interpreted in terms of size inequality of growing polymer molecules and LC solvent²⁻⁴. The special role of cross-linking has hardly been addressed, although its importance as a driving force for phase separation has been well recognized in the past^{5,6}. In addition to the step reactions mentioned above, chain cross-linking copolymerization of monoacrylates and polyfunctional acrylates is also widely used to induce the desired phase separation^{2,7,8}. As opposed to epoxide/amine systems, the acrylates are characterized by gelation early in the reaction⁹. Cross-linking-induced phase separation is therefore expected to be the dominant process. Additional cross-linking rather than gelation is necessary to stabilize the desired morphology of small LC droplets in a continuous matrix. Optimal conditions are generally obtained through trial and error. In view of the large number of parameters involved, this is a rather cumbersome process. Therefore, it is desirable to understand the relationship between the molecular structures of the monomer/oligomer and the LC compounds and the curing conditions on the one hand, and the morphology and the electro-optical performance of the system on the other hand. However, practical LC systems are generally mixtures composed of seven or more components, in order to extend the temperature range of existence of the LC phase. As different components have different solubilities in the crosslinked polymer and since a significant part of the LC mixture remains dissolved in the matrix³, the composition of the phase-separated, electrically active fraction of the LC will be different

* To whom correspondence should be addressed

from its initial composition¹⁰. Moreover, practical monomer systems not only contain simple monomers but also (generally rather impure) oligomers^{2,7,8}. At present it does not seem feasible to arrive at a complete description of technical systems. Therefore, we have chosen to investigate simple model systems consisting of one or two monomers and a single LC compound, and to compare the results with those obtained on systems of technical importance.

In this paper, we will report some preliminary experiments in which the onset of turbidity and the progress of the chemical reaction are monitored simultaneously by laser transmission and photo-d.s.c., respectively. Our primary aim is to show that subtle changes of the LC or polymer structure or concentration strongly influence the extent of polymerization at which turbidity appears. The latter is related to the final morphology and to the electro-optical response. The relation between initial composition, phase separation, morphology and electro-optical performance will be discussed in forthcoming papers^{11,12}. The required thermodynamic framework will also be published separately¹³. Additional insight into the development of the morphology was obtained by light microscopy during u.v. exposure. This methods revealed the occurrence of secondary phase separation, i.e. the formation of droplets inside droplets already formed. It is speculated that this effect might be responsible for part of the observed hysteresis. A secondary aim of this paper is to show the versatility of laser-equipped photo-d.s.c.; it not only enables the measurement of conversion at the onset of turbidity, the simple recording of transmission-temperature curves also yields cloud points which may be used in the construction of phase diagrams. A special cell design allows the measurement of transmission-voltage curves of d.s.c. samples after polymerization.

Experimental

Chemicals, model system and technical system. Tetraethylene glycol diacrylate (TEGDA) and decanediol dimethacrylate (DDDM) were obtained from Polysciences, and 2-ethoxyethyl acrylate (EEA) was obtained from Aldrich. Monomers were used without further purification. Dimethoxyphenylacetophenone (Irgacure 651), used as a photoinitiator, was obtained from Ciba Geigy. The technical LC mixture TL202 and the compounds K15 (n-pentylcyanobiphenyl) and K24 (n-octylcyanobiphenyl), as well as the technical mixture of acrylates PN393, were obtained from Merck (Poole, UK). Structural formulae are shown in Figure 2. The clearing points (nematic to isotropic transitions) of K15 and K24 are 35 and 41°C, respectively.

Modified photo-d.s.c. for simultaneous monitoring of rate and extent of polymerization and turbidity. Figure 1 shows schematically the modifications of a Perkin Elmer DSC7 differential scanning calorimeter. The conversion into a photo-differential scanning calorimeter has been described¹⁴. The 4 W Philips TL08 lamp was replaced by a 10 W Philips PL 10 lamp. This lamp consists of two cylindrical fluorescent tubes, spaced at about 3 mm. On top of the calorimeter a 4 mW HeNe laser (Spectra-Physics) and a beam splitter are mounted, together with a pair of Centronic silicon photodetectors (type OSD, saturation level 5 W cm⁻²) for monitoring the intensities

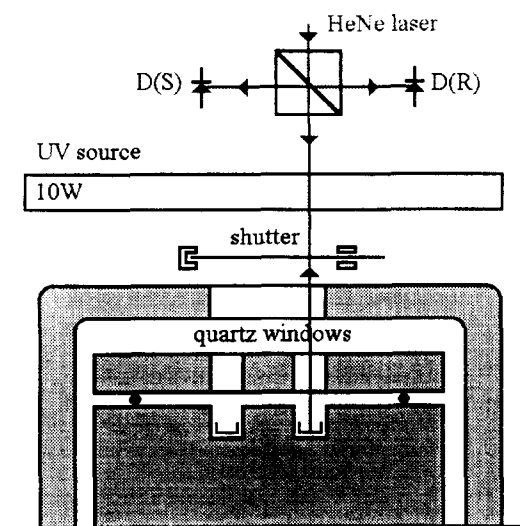


Figure 1 Laser photo differential scanning calorimeter set-up

of the primary (reference) beam and the sample beam. The latter passes between the lamp tubes and through the shutter to the sample. Either a silicon mirror is placed under a glass sample substrate or a silicon substrate is used. In both cases, the sample beam is transmitted through the sample twice. The diode currents are converted to a voltage and their ratio is fed into a personal computer. Neutral density filters are used to bring the intensity down from the maximum value of 8 mW cm⁻² to the desired level. At 2 mW cm⁻² or less a shutter with a small hole allowing the laser beam to pass to the sample without significant u.v. exposure can be used. This allows recording and adjustment of the baseline before opening the shutter.

Light microscopy during photopolymerization. A Leitz-type Aristomet 020504 polarizing microscope was used at 200 times magnification. A polyimide foil (Kapton from Dupont) protected the sample from u.v. light emitted by the sample illumination lamp. Samples were contained in a thermostatted box (Linkam THMSE 600). U.v. exposure was carried out using a high-pressure mercury exposure arc provided with a glass optical fibre output (Efos Ultracure 100), directed towards the sample. Intensities ranged from 0.08 to 8 mW cm⁻².

Sample preparation. Monomer solutions contained 1–3 wt% of photoinitiator. Mixtures with LC were prepared by weighing. For transmission photo-d.s.c. the conventional sample pans or their lids are inadequate; their specular reflectivity is too low due to surface roughness. Instead, thin slices of silicon (thickness 200 μm, diameter 7 mm) can be used. Alternatively, the sample solution was sandwiched between two thin glass discs of the same diameter coated with optically transparent and electrically conducting indium-tin oxide (ITO). The discs were D shaped, i.e. circles from which a segment of about 1 mm height had been removed. They were mounted with their straight sides opposite each other, in order to enable electrical connection after mechanical fixation with respect to each other by the polymerization of the monomers. Fibreglass spacers with a thickness of 18 μm were either added to the sample solution or deposited

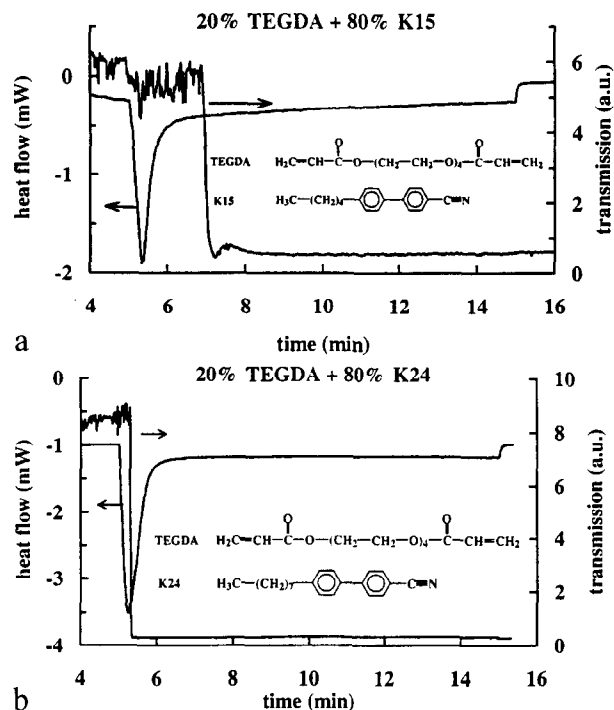


Figure 2 (a) Photo-d.s.c. and turbidity curves of TEGDA/K15. (b) Photo-d.s.c. and turbidity curves of TEGDA/K24

onto the substrate by spincoating from a slurry in ethanol.

Electro-optical characterization. The measurements of the electro-optical characteristics of PDLC cells were performed on a modified Display Measuring System from Autronic GmbH (Karlsruhe, FRG). The cells are illuminated by a narrow white light beam with a divergence of 1.5° . The full collection angle is 5.2° . The intensity of the transmitted light is measured with a photomultiplier. Addressing is achieved with a square wave ($f = 1 \text{ kHz}$), and the increase of voltage as function of time is 0.05 V s^{-1} . All measurements were performed at room temperature.

Results and discussion

Nematic phase formation. Figure 2 shows the photo-d.s.c. and laser transmission curves of TEGDA/K15. The heat of reaction can be obtained from integration of the d.s.c. curve; it is proportional to the extent of double bond conversion¹⁴. It can be seen that most of the heat of reaction has been liberated before the sample becomes turbid (transmissions are given in arbitrary units). The Flory-Huggins interaction parameter χ is not known for this system but a crude estimate based on group contributions¹⁵ gives a value for the solubility parameters $\delta = 21.7 \text{ J}^{1/2} \text{ cm}^{-3/2}$ for poly(TEGDA) and $\delta = 21.0 \text{ J}^{1/2} \text{ cm}^{-3/2}$ for K15. From these values the enthalpic part of χ may be equated: $\chi_H = V_1(\delta_1 - \delta_2)^2/RT$ in which V_1 is the molar volume of the LC solvent. This yields $\chi_H = 0.06$. Unfortunately, the entropic contribution to χ cannot be obtained in this way.

Variation of LC structure. The effect of introducing a small change in the structure of the LC compound is illustrated in Figure 2b. Increasing the length of the

aliphatic group causes the phase separation to occur much earlier in the reaction, at about 44% double bond conversion. The value of the interaction parameter was estimated in the same way as above: $\chi_H = 0.20$. The trend in χ_H shows a reduced compatibility between LC and polymer in going from K15 to K24, and this immediately shows up as an earlier development of turbidity. It must be emphasized that this ranking of the χ values is rather arbitrary since the entropic contributions are not known and there is no good reason for assuming these to be constant.

Variation of LC content. The effect of changing the initial composition of the mixture is illustrated in Table 1: the higher the monomer concentration, the higher the double bond conversion required for the observation of phase separation. At 50% monomer the sample remains clear; there is enough polymer to dissolve the LC completely.

Table 1 Extent of conversion of TEGDA/K15 at incipient turbidity^a

| TEGDA (wt%) | C = C conversion | |
|-------------|--------------------------|-----------------------|
| | 0.08 mW cm^{-2} | 8 mW cm^{-2} |
| 5 | 0.50 | 0.37 |
| 10 | 0.58 | 0.41 |
| 20 | 0.78 | 0.56 |
| 50 | — | — |

^a Assuming complete conversion of double bonds at the end of the polymerization. Temperature of polymerization: 20°C

Variation of light intensity. The data in Table 1 also show that a high light intensity favours an early phase separation. We have no conclusive explanation for this phenomenon. It could be related to the well-known formation of inhomogeneities or microgel particles during the chain cross-linking polymerization of divinyl monomers such as TEGDA^{9,16}. Microgel particles reduce the number of elastically effective cross-links, thereby postponing phase separation. At a higher intensity a more homogeneous system will be formed, and so phase separation will take place earlier in the reaction.

Variation of cross-link density. The influence of cross-link density is illustrated in Table 2. Here the cross-link density of the polymer was reduced while

Table 2 Extent of conversion of TEGDA/EEA/K15 at incipient turbidity^a

| [TEGDA] (wt%) | [EEA] (wt%) | C = C conversion at 8 mW cm^{-2} |
|---------------|-------------|-------------------------------------------|
| 20 | 0 | 0.56 |
| 18 | 2 | 0.65 |
| 16 | 4 | 0.76 |
| 10 | 10 | 0.84 |
| 5 | 15 | 0.90 |
| 0 | 20 | 0.95 |

^a Assuming complete conversion of double bonds at the end of the polymerization. LC content: 80%. Temperature of polymerization: 20°C

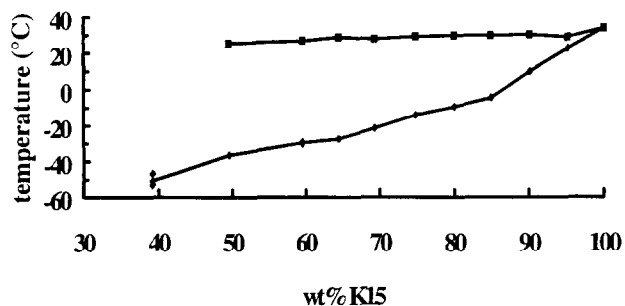


Figure 3 Cloud points of TEGDA/K15 mixtures before (diamonds) and after (squares) polymerization

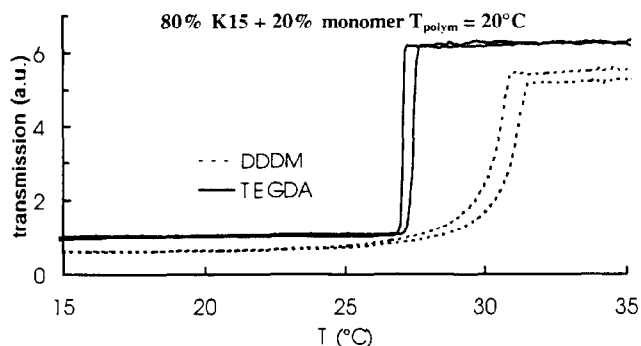


Figure 4 Transmission-temperature curves for poly(TEGDA)/K15 and poly(DDDM)/K15

keeping the LC concentration constant by replacing part of the TEGDA with EEA.

In this way the chemical composition of the polymer was varied as little as possible; the cross-link density is the main variable. A lower cross-link density requires a higher conversion for turbidity to show up. At 0% cross-linker, size-induced phase separation will occur, although some degree of cross-linking by chain transfer cannot be excluded.

Nematic phase formation versus liquid-liquid demixing. It should be noted that the onset of

turbidity does not necessarily coincide with the onset of phase separation: strong turbidity only occurs in the nematic state, that is at a high purity of the LC phase. In principle, isotropic droplets may be formed first which later turn nematic due to monomer consumption. So far, this has only been observed in TEGDA/K15 at low monomer (high LC) contents. At < 10% TEGDA, first the formation of isotropic droplets was observed under the polarizing microscope, and later on these droplets turned nematic. In all other cases the droplets were nematic as soon as they appeared under the microscope. Microscopy and the optical transmission/photo-d.s.c. are obviously complementary methods.

Measurements of cloud points. The present set-up may also be used to study the phase diagram of the system before and after polymerization, using cloud point measurements obtained from thermal scans at a given composition. Some results obtained on cooling TEGDA/K15 are shown in Figure 3. The lower curve shows the cloud points of monomer/LC mixtures. The location of the isotropic to nematic transition with respect to the transition in the pure LC is a measure of the purity of the LC phase obtained. The lower the LC content, the lower its transition temperature. The upper curve shows the transition temperatures after polymerization. During polymerization they increase to values close to the value of pure LC. This shows that almost pure LC remains after the reaction.

Transmission-temperature curves. Figure 4 shows the dependence of the transmission on temperature, for two systems: K15 with TEGDA and K15 with DDDM. TEGDA shows a sharp thermal transition slightly below the clearing temperature of the pure LC and significant undercooling during the reverse thermal scan. DDDM on the other hand shows a much more gradual response. This might be indicative of the presence of a wide distribution of LC domain sizes with a strongly size-dependent transition temperature. A similar effect has been observed with the melting of unreacted monomer in a densely cross-linked network¹⁷. However, this could not be confirmed by microscopy since, at the end of the

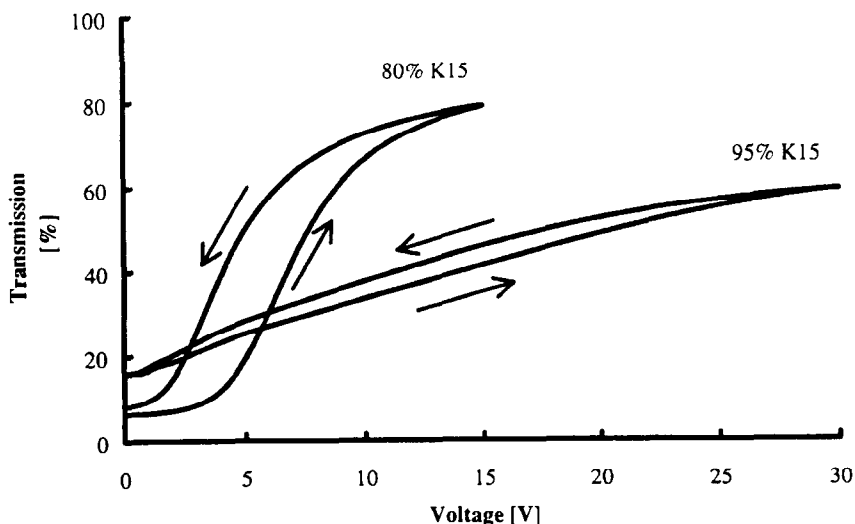
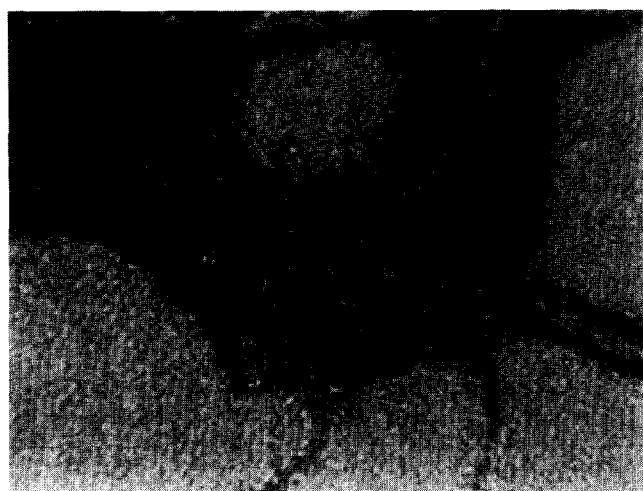
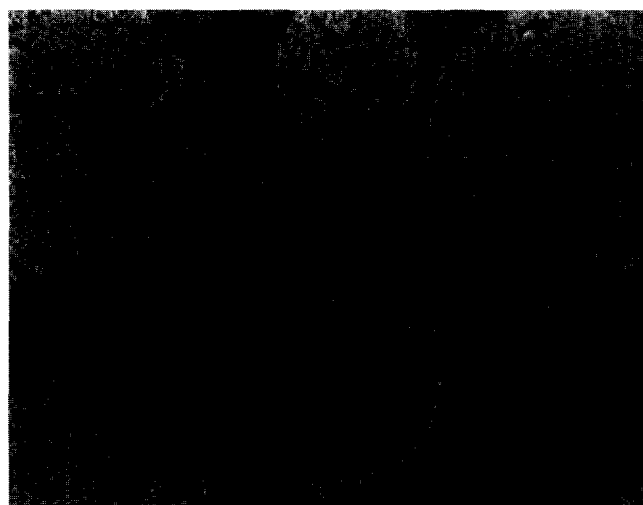


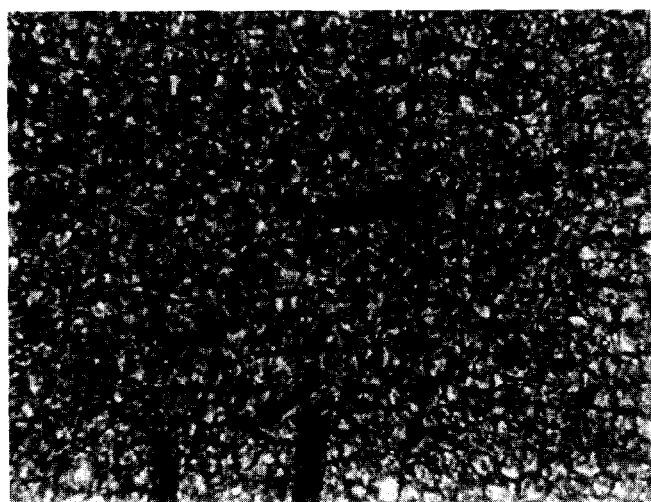
Figure 5 Transmission-voltage curves for poly(TEGDA)/K15. The 95% K15 curves were obtained from an aged d.s.c. sample with 18 μm spacers, and the 80% K15 curves were from a regular cell with 7 μm spacers



(a) 0°C 0.08 mW/cm² 100 μm



(b) 0°C 0.8 mW/cm² 100 μm



(c) 25°C 0.8 mW/cm² 100 μm

Figure 6 Phase separation in a system composed of acrylates (20% PN393) and an LC mixture (80% TL202). Straight bars are glass spacers with a diameter of 18 μm. (a) 0°C, 0.08 mW cm⁻². (b) 0°C, 0.8 mW cm⁻². (c) 25°C, 0.8 mW cm⁻²

reaction, no isolated droplets are observed but rather two co-continuous phases.

Transmission-voltage curves. The use of small cells with transparent electrodes in the differential scanning calorimeter allows the subsequent electro-optical characterization of the sample formed under well-defined conditions. *Figure 5* shows the transmission-voltage curves for poly(TEGDA)/K15. At the highest LC concentration used, 95%, droplets no longer formed. The response does not show any discrete switching behaviour. At 80% LC a droplet-like structure is observed under the microscope and a switching threshold is seen. A pronounced hysteresis occurs at both concentrations. This shows that our simple model system may perhaps throw some light on the basic phase separation phenomena, but also that it is far from useful in switching applications. The hysteresis in particular requires further investigation. At present this effect is poorly understood. One possible cause might be a secondary phase separation, i.e. the formation of

polymer gel in LC droplets already formed. This is expected to increase the local viscosity and thereby the response time of the system.

Secondary phase separation. *Figure 6a* shows a picture of the phase separation in a commercial system composed of acrylates (20% PN393) and an LC mixture (80% TL202). It was polymerized at 0°C. This system demixed thermally before the u.v. light was switched on. Upon polymerization at a light intensity of 0.08 mW cm⁻², new, much smaller domains were formed. *Figure 6b*, shows a similar experiment carried out at a higher light intensity: 0.8 mW cm⁻²; here, too, new domains were formed. A secondary phase separation occurs within the large domains already present before polymerization: thread-like structures develop. Obviously, there is insufficient time for complete demixing of new polymer formed in the large LC domains. At the low light intensity used in *Figure 6a* no such effect was observed, the large domains appear to be pure, whereas the smaller, newly formed domains are

evenly spaced in between the large ones. Around the large circular domains already present before polymerization in *Figure 6b*, a series of new small LC domains can be seen. They are found at an approximately constant distance from the large ones. Either an LC concentration gradient already existed around the large domains before polymerization, or it was generated by a rapid expulsion of LC and perhaps some polymer from the large LC-rich domains.

If the same system is polymerized at a higher temperature, 25°C, the image shown in *Figure 6c* appears. Starting from a clear solution, an entirely different morphology is formed. No secondary phase separation could be observed. Nevertheless, it seems not unlikely that it has occurred here also, albeit on a much smaller spatial scale: in any LC droplet containing monomer and initiator as impurities, initiation and polymer growth may take place, followed by replenishment of consumed monomer by diffusion. Polymeric threads inside LC domains as shown in *Figure 6b* might be responsible for the rather slow relaxation of LC orientation in an electric field. These three figures illustrate that both the temperature of polymerization and the rate of polymerization, which is controlled by the light intensity, are very important parameters with respect to the morphology. It should be noted that in real devices much smaller droplets are used; the ones shown here just serve to illustrate the secondary phase separation. Secondary phase separation has not only been observed in droplets formed by cooling before polymerization but also under purely isothermal conditions^{4,18}.

Conclusion

A laser-equipped photo-differential scanning calorimeter enables location of the onset of turbidity with respect to the progress of a polymerization process. At constant overall composition (e.g. constant monomer conversion) the cloud point can be obtained from a temperature scan. The onset of turbidity is caused by the appearance of a nematic phase. The extent of conversion at which it occurs during isothermal polymerization is shown to be very sensitive to the initial LC content, LC

structure, monomer structure and cross-link density of the polymer. The same applies to the temperature at which turbidity appears before cooling at constant overall composition. The conversion at which turbidity appears during polymerization also depends on the rate of polymerization. The photo-d.s.c./turbidity method is useful for the study of the relation between structure and preparation of PDLCs by polymerization and their electro-optical performance. Light microscopy has revealed the occurrence of secondary phase separation in acrylate/LC mixtures.

References

- 1 Doane, J. W. in 'Liquid Crystals. Applications and Uses' (Ed. B. Badur), World Scientific, Singapore, 1990, Ch. 14, p. 361
- 2 Hirai, Y., Niiyama, S., Kumai, H. and Gunjima, T. *Rep. Res. Lab., Asahi Glass Co., Ltd* 1990, **40**, 285 (*SPIE* 1990, **1257**, 2)
- 3 Smith, G. W. *Int. J. Mod. Phys. B* 1993, **7**, 4187
- 4 Kim, J. Y., Cho, C. H., Palfy-Muhoray, P., Mustafa, M. and Kyu, T. *Phys. Rev. Lett.* 1993, **71**, 2232
- 5 Dušek, K. *J. Polym. Sci.* 1967 **C16**, 1289
- 6 Dušek, K. in 'Polymer Networks—Structure and Mechanical Properties' (Eds A. J. Chomppf and S. Newman), Plenum Press, New York, 1971, p. 245
- 7 Fujisawa, T., Ogawa, H. and Muruyama, K. *Jpn Display* 1989, **89**, 690
- 8 Noh, C. H., Jung, J. E., Sakong, D. S. and Choi, K. S. *Mol. Cryst. Liq. Cryst.* 1993, **237**, 299
- 9 Dušek, K. in 'Developments in Polymerisation-3' (Ed. R. N. Haward), Applied Science, London, 1982, Ch. 4
- 10 Nolan, P., Tillin, M. and Coates, D. *Mol. Cryst. Liq. Cryst. Lett.* 1992, **8**, 129
- 11 Serbutoviez, C., Kloosterboer, J. G., Boots H. M. J. and Touwslager, F. J. *Macromolecules* in press
- 12 Serbutoviez, C., Kloosterboer, J. G., Boots H. M. J. and Touwslager, F. J. *Liquid Crystals* in press
- 13 Boots, H. M. J., Kloosterboer, J. G., Serbutoviez, C. and Touwslager, F. J. *Macromolecules* in press
- 14 Kloosterboer, J. G. and M. Lijten, G. F. C. *ACS Symp. Ser.* 1988, **367**, 409
- 15 Van Krevelen, D. W. 'Properties of Polymers', 3rd edn, Elsevier, Amsterdam, 1990, Ch. 7
- 16 Kloosterboer, J. G., Van de Hei, G. M. M. and Boots, H. M. J. *Polym. Commun.* 1984, **25**, 354
- 17 Kloosterboer, J. G., Van de Hei, G. M. M. and Lijten, G. F. C. M. in 'Integration of Fundamental Polymer Science and Technology' (Eds L. A. Kleintjens and P. J. Lemstra), Elsevier Applied Science, London, 1986, p. 198
- 18 Kloosterboer, H., Serbutoviez, C., Boots H. and Touwslager, F. *Polym. Mater. Sci. Eng.* 1996, **74**, 190